

Nanoscale

Accepted Manuscript



This is an *Accepted Manuscript*, which has been through the Royal Society of Chemistry peer review process and has been accepted for publication.

Accepted Manuscripts are published online shortly after acceptance, before technical editing, formatting and proof reading. Using this free service, authors can make their results available to the community, in citable form, before we publish the edited article. We will replace this *Accepted Manuscript* with the edited and formatted *Advance Article* as soon as it is available.

You can find more information about *Accepted Manuscripts* in the [Information for Authors](#).

Please note that technical editing may introduce minor changes to the text and/or graphics, which may alter content. The journal's standard [Terms & Conditions](#) and the [Ethical guidelines](#) still apply. In no event shall the Royal Society of Chemistry be held responsible for any errors or omissions in this *Accepted Manuscript* or any consequences arising from the use of any information it contains.



Journal Name

ARTICLE

High Performance Carbon Nanotube – Polymer Nanofiber Hybrid Fabrics

Ozkan Yildiz^a, Kelly Stano^a, Shaghayegh Faraji^a, Corinne Stone^b, Colin Willis^b, Xiangwu Zhang^a, Jesse

S. Jur^a, and Philip D. Bradford*^a

Received 00th January 20xx,
Accepted 00th January 20xx

DOI: 10.1039/x0xx00000x

www.rsc.org/

Stable nanoscale hybrid fabrics containing both polymer nanofibers and separate and distinct carbon nanotubes (CNTs) are highly desirable but very challenging to produce. Here, we report the first instance of such a hybrid fabric, which can be easily tailored to contain 0-100% millimeter long CNTs. The novel CNT – polymer hybrid nonwoven fabrics were created by simultaneously electrospinning nanofibers onto aligned CNT sheets which were drawn and collected on a grounded, rotating mandrel. Due to the unique properties of the CNTs, the hybrids show very high tensile strength, very small pore size, high specific surface area and electrical conductivity. In order to further examine the hybrid fabric properties, the hybrids were consolidated under pressure, and also calendered at 70 °C. After calendering, the fabric's strength increased by an order of magnitude due to increased interactions and intermingling with the CNTs. The hybrids are highly efficient aerosol filters; consolidated hybrid fabrics with a thickness of 20 microns and areal density of only 8 g/m² exhibited ultra-low particulate (ULPA) filter performance. The flexibility of this nanofabrication method allows for the use of many different polymer systems which provides the opportunity for engineering a wide range of nanoscale hybrid materials with desired functionalities.

1. Introduction

Due to their small fiber diameter, high specific surface area, high porosity and small pore sizes, polymer nanofiber nonwovens produced via electrospinning have gained attention in a broad range of applications such as aerosol and liquid filtration¹⁻⁴, protective garments⁵, barrier membranes⁶, tissue scaffolds⁷, catalyst support structures, and others⁸⁻¹². These applications require well defined nonwoven properties such as pore diameters, internal surface area, permeability, as well as high mechanical strength^{8,10}. However, nanofiber nonwovens typically exhibit low individual fiber and web mechanical strength compared to conventional nonwovens due to their highly porous structure, intrinsically low or, random fiber orientation, weak bonding between nanofibers and low polymer orientation within individual nanofibers. These structural parameters hinder their performance and use in many applications^{9,10,13,14}. The result is that nanofiber nonwovens are supported and adhered to a base fabric composed of macroscopic fibers.

To avoid the use of a base fabric, previous studies have

reported several methods to improve nanofiber mechanical strength^{9,10,15}. These routes include: changing the nonwoven nanofiber mat into self-bundled yarns^{9,16}, applying surface modification or post treatments such as stretching, twisting, or annealing¹⁷⁻²¹, and reinforcing the single nanofiber strength by adding carbon nanotubes (CNTs)^{9,16,22}, layered silicates²³ or graphite nanoplatelets²⁴ into the polymer spinning solution. Many of these approaches either change the highly porous nature of nanofiber nonwovens or complicate the electrospinning process. Among these methods however, the addition of CNTs to polymer electrospun fibers has attracted many researchers due to their high mechanical, electrical and multifunctional properties and strong interactions with electrospun fiber matrices resulting in large interfacial area^{7,25-30}. However, several factors significantly influence the final nanofiber nonwovens properties, such as CNT dispersion, orientation, alignment, volume (or weight) content, and interfacial adhesion with polymer^{25,31-36}. Above the CNT electrical percolation threshold, additional CNTs can cause a bead structure formation which negatively affects the mechanical properties of the nanofiber nonwovens^{25,26}. Since CNTs usually exist as stable bundles and their dispersion and alignment in polymer matrices are very difficult to achieve due to strong van der Waals interactions among CNTs, several different processing methods have to be applied to disperse CNTs such as high power ultrasonic mixer functionalization or the addition of coupling agents or surfactants^{25,31,34,35,37-39}. Another disadvantage of using this method is the limitation of the CNTs content in polymer solutions. When the

^a Department of Textile Engineering Chemistry and Science, North Carolina State University, Campus Box 8301, Raleigh, NC USA 27695

^b Defence Science and Technology Laboratory, Salisbury, Wiltshire SP4 0JQ, UK

† Electronic Supplementary Information (ESI) available: [details of any supplementary information available should be included here]. See

DOI: 10.1039/x0xx00000x

CNT weight or volume fraction is higher than approximately 1-5% in polymer solution, the mechanical properties of nanofiber nonwovens decrease and become lower than pure polymer samples^{25,28,39-42}. In order to address these limitations and to improve final nanofiber nonwoven properties, new processing techniques are needed where CNTs can be utilized in high concentrations, dispersed homogeneously and aligned in preferential directions.

Continuous CNT sheets are excellent candidates for producing nanofiber nonwoven fabrics due to their high surface area, alignment, electrical conductivity and mechanical properties⁴³⁻⁴⁵. In this work, a novel CNT – polymer hybrid nonwoven fabric is created by simultaneously electrospinning PEO nanofibers onto aligned CNT sheets, which are drawn and collected on a grounded, rotating mandrel. PEO polymer solution was chosen for electrospinning because it is easily electrospun, and melts at low temperature. However any polymer that can be electrospun should be able to be integrated with the CNT webs to form the same hybrid fabrics. As a result of this novel hybridization method, continuous electrospun polymer nanofibers are fully integrated among the aligned CNT sheets (diameter ~30 nm, aspect ratio ~50,000) trapping them inside the fabrics. Due to the unique properties of CNTs, the hybrid fabrics show very high strength, small pore size, high specific surface area and electrical conductivity. This novel process demonstrates a new technology which overcomes the numerous physical and mechanical limitations of traditional electrospun nonwovens, and is promising for some of the most demanding nanofiber applications. In this article, the mechanical, electrical, aerosol filtration, permeability, and barrier properties of the novel hybrid fabrics are evaluated.

2. Experimental

2.1 CNT Synthesis

Vertically aligned multi-walled carbon nanotubes (MWCNT) were grown by chemical vapor deposition (CVD) on a quartz substrate using iron II chloride (FeCl_2) as the catalyst⁴⁴. First, iron chloride and substrate were placed inside a quartz tube. Then this inner tube was loaded into outer quartz tube of a horizontal tube furnace. The chamber was sealed and pumped to less than 10 mTorr, and then the chamber was heated to 760°C. When the chamber's temperature reached 760°C, the growth gasses, acetylene (600 sccm), argon (395 sccm) and chlorine (5 sccm), were introduced into the chamber. The reaction took place 20 min, after which time the chamber was returned to starting conditions (ambient temperature and atmospheric pressure). CNT array height (and corresponding CNT length) was approximately 1 mm. The aligned CNT sheets were formed by dragging a razor blade across one edge of the CNT array. Clean CNT surfaces and sufficient van der Waals interactions between tubes creates an attraction between tubes to allow them to be transferred from the aligned vertical orientation in the CNT array to the aligned horizontal orientation in the CNT sheet. After starting the drawing process, the CNT sheet was attached to the mandrel and wound during the electrospinning process. The sheet continued to be taken up until all CNTs in the array were consumed. CNT arrays used in this study had dimensions of 60 mm

x 100 mm which translated to approximately 30 m length of 60 mm wide aligned CNT sheet.

2.2 Electrospinning Process and Characterization

PEO of M_w 600,000 was purchased from Sigma Aldrich. A 5% weight fraction of PEO solution was prepared by mixing PEO in water and then stirring for 1 day. When PEO was completely dissolved in water, the polymer solution was loaded into a 10 mL syringe with luer-lock connection and used in conjunction with a 1.27 cm, 21 gauge blunt tip needle. The electrospinning apparatus included a syringe pump from New Era Pump Systems (model NE-300), which operated at a flow rate of 1 mL/h. The high voltage power supply was from Gamma (High Voltage model ES40P-20W/DAM). The operating voltage varied from 10 to 15 kV and the distance between the collector and needle was 15 cm. The mandrel served as one of the electrodes in the electrospinning process and the mandrel was rotated by a Regulated DC Power Supply (model DICKI 360). Different CNT weight fraction samples were produced by changing the winding speed during electrospinning. The surface morphology of CNT – polymer hybrid nonwoven fabrics was examined using a FEI XHR-Verios 460L Field Emission SEM with a beam voltage of 1.0 kV. All samples were imaged as-prepared without sputter coating.

Once the samples were prepared, two additional processing steps were completed to understand the effect of hybrid fabric structure on the properties. The first was to consolidate the fabric under 2 MPa of pressure without heat treatment for 5 min. The second was to calender the samples at 70 °C and 2 MPa pressure for 5 min.

2.3 Physical Testing

In order to understand the effect of super aligned CNTs on the physical properties of hybrid fabrics, their mechanical and electrical conductivity properties were evaluated. Samples with dimensions of 40 mm x 4 mm were cut along the longitudinal CNT direction by sharp blade without damaging hybrid fabric. The thickness of the samples was measured by micrometer. Tensile strength of the samples was tested using a Shimadzu EZ-S instrument with a 100 N load cell. Before testing, samples were mounted to paper tabs with tape on both sides to prevent slipping and reduce stress concentration at the grips. The gauge length of the tensile hybrid samples was 20 mm and testing speed was 0.5 mm/min. Electrospun fabric strength is sometimes calculated from fiber cross-sectional area only (based on the mass of sample and density of the fibers)^{28,40} which gives inflated strength values. In this work, engineering stress was determined by dividing the load on the fabric by the fabric cross sectional area calculated using the measured fabric thickness.

A four probe resistance measurement system was used to measure electrical properties of the samples. Samples with dimensions of 0.5 cm x 4 cm were placed onto a glass plate with four parallel gold electrodes across it. To ensure good contact between the sample and the gold electrodes, a square shaped piece of glass and a 500 g weight were placed on top of the samples during the measurements.

2.4 Aerosol Filtration Testing

The filtration properties of the hybrid fabrics were tested using a TSI Model 3160 Automated Filter Tester. The filtration efficiency of the control sample (eight layers of PEO electrospun fabric that was produced at lower mandrel speed) and seven layer hybrid fabrics (CNT weight fraction of 15%, 30% and 60%) were evaluated at 15 cm/s face velocity. DOP (dioctyl phthalate) particles with diameters between 0.010 and 0.3 microns were generated by a collision type atomizer and evaporated through a membrane dryer, and then neutralized by a Kr-85 radioactive source. The neutralized DOP aerosol particles were fed into the filter holder with an effective area of 6.45 cm² and their number concentrations measured upstream and downstream of the hybrid fabric by using two condensation particle counters (CPCs, TSI, Model 3760A). The collection efficiency was calculated using the following equation:

$$E = 1 - \frac{C_{down}}{C_{up}} = 1 - P \quad \text{Equation (1)}$$

where, E is the fractional efficiency of a specific size of DOP particles, C_{down} and C_{up} are the number concentration of particles on the downstream and upstream sides, and P is the particle penetration fraction.

2.5 Plasma Functionalization

In order to make oleophobic polymer-CNT hybrid fabrics, a low surface energy chemical, PFAC8 (C₈F₁₇CH₂CH₂OCOCH=CH₂, Fluorochem, Derbyshire, UK) was deposited onto the CNT-polymer hybrid fabrics by using pulsed plasma polymerization. The treatment were carried out in a inductively coupled glass cylindrical glow discharge reactor, (10 cm diameter, 4.3x10⁻³ m³ volume, 1x10⁻² mbar base pressure) connected to a vacuum pump via a liquid nitrogen cold trap. First, the hybrid fabric was placed on a glass slide which was then placed in the centre of the coils. The chamber was then evacuated to the base pressure of the apparatus, typically

1 x 10⁻² mbar. Once base pressure had been reached, the PFAC8 vapour was introduced into the reactor. The reactor was purged with the vapour for five minutes, and once the the pressure is stabilised at 8 x 10⁻² mbar, the radio frequency (RF) generator was switched on to create a 40W continuous wave plasma. This was allowed to run for 10 seconds. At this point the pulse generator was turned on, at a pulsing sequence of 40µs on, 20ms off. Once a stable plasma deposition rate was established (indicated by uniform pulse envelope, using an RF probe and oscilloscope), the polymerization was allowed to run for two minutes. At the end of the treatment the RF generator was switched off and the reactor purged for 2 minutes with PFAC8 vapour, prior to being evacuated back to base pressure. Once base pressure was reached, the vacuum chamber was isolated from the pump, the system brought up to atmospheric pressure and the samples then removed.

2.6 Moisture Vapor Transmission Rate (MVTR) Test

Moisture vapor transmission rate of hybrid fabrics were measured following ASTM E96 test method by using a MVTR tester machine in standard test condition lab (20°C, 65% relative humidity). The hybrid fabrics were sandwiched between two aluminum foil discs (adhesive on one side) that had a punched hole (3.81 cm diameter) in the center. This assembly was sealed in a metal dish (64 mm diameter and 13 mm in depth) filled with 10 g of water. A vibration free turn table carrying 8 dishes rotated uniformly at 5 meters per minute to insure that all samples were exposed to the same average ambient conditions during the test. The assembly specimen in the metal dishes were allowed to stabilize for two hours before taking the initial weight. The specimens were weighed again after a 24 hours interval. The moisture vapor transmission rate (MVTR) was then calculated in units of g/m²-24 hours. The MVP of the hybrid fabrics is determined by normalizing the MVTR results.

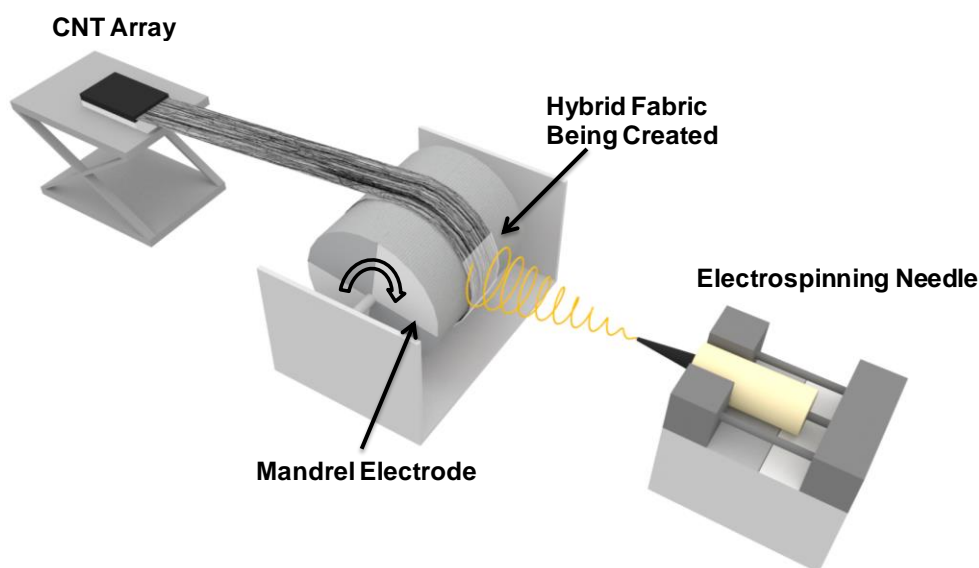


Fig. 1 Schematic of the hybrid fabric production process where electrospun fibers are taken up simultaneously with aligned CNT sheets.

2.7 Contact Angle Measurements

Contact angle measurements were made using a DropShape Analyser 100 (DSA100, Krüss, Germany). Probe liquids were water, hexadecane, ethylene glycol and di-iodomethane (Aldrich UK, except for the water). Contact angle measurements were made using the built in software.

3. Results

3.1 Hybrid Fabric Preparation

Figure 1 shows a schematic of the process that has been developed. In this novel process, the aligned CNT sheet is taken up onto an electrically conductive mandrel. This mandrel serves as one of the electrodes in the electrospinning process. As the mandrel rotates, the CNT sheet is taken up and at the same time covered with a layer of electrospun nanofibers.

Figure 2 shows an actual picture of the hybridization process, photographic images of the CNT – polymer hybrid nonwoven fabrics and SEM images of representative samples. One of the additional advantages of this process is that the 1 mm long CNTs become trapped by the polymer fiber layers, encapsulating them in the fabric. This significantly reduces the likelihood of CNTs escaping into the environment^[44]. The mass fraction of the CNTs in the hybrid fabrics is easily controlled anywhere from 0-100% by adjusting the mandrel take-up speed during the process. Slower speed allows for more electrospun fibers to build up while higher speed allows for less polymer fibers to build up. Figure 2b shows a picture of five different samples; two control samples (0% CNTs and 100% CNTs)

and samples where the CNT mass fraction was approximately 15%, 30% and 60%. Once the samples were made, we also completed two additional processing steps to understand their effect on the hybrids' properties. The first was to consolidate the fabric under pressure but no heat. The second was to calender the sample at 70 °C under pressure. Figures 2c-d show SEM images of the 30% CNT hybrid fabric's morphology before and after heated calendaring, respectively. Before calendaring, the separate components of the hybrid structure can be clearly seen. The electrospun nanofibers had an average diameter of 250 nm while the CNTs had an average diameter of 30 nm. After heat pressing, a new morphology was created. At low CNT weight fractions, a solid composite film was created. When the CNT weight fraction was high, a porous CNT fabric with melted fiber bond points was created. Surprisingly, a majority of the fabric still retained the individualized CNT structure

3.2 Physical Test Results

The mechanical properties of CNT – polymer hybrid nonwoven fabrics were investigated using a Shimadzu mechanical tester. The results are shown in Figure 3a. The pure PEO electrospun material exhibited low mechanical properties that were similar to others found in the literature^[26,29,46]. While it is no surprise that the CNTs would reinforce the hybrid fabrics, the level of reinforcement was unexpected. The 15% CNT hybrid fabric showed the highest mechanical properties and had a tensile strength which was 15% higher than the electrospun control sample. Above 15% CNTs, the tensile strength gradually decreased but was still over an order of magnitude higher than the electrospun control. The tensile

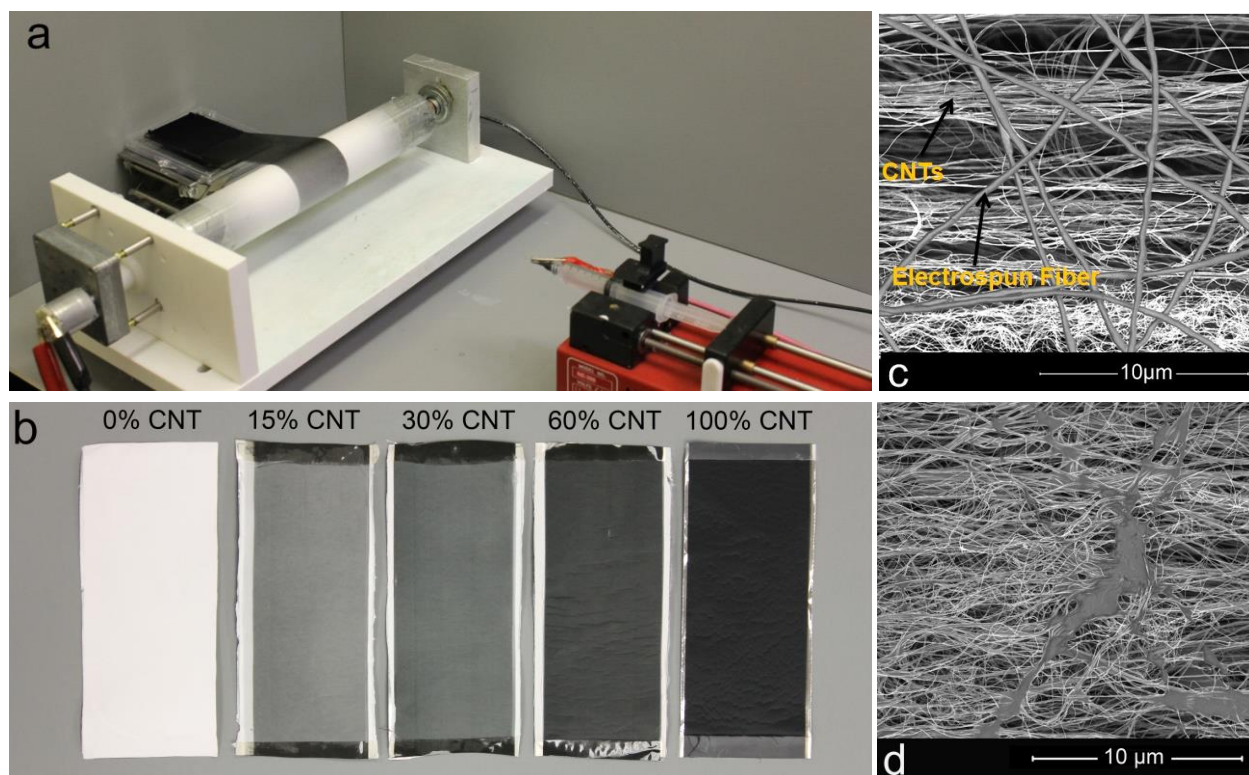


Fig. 2 a) Setup of the hybrid nanofiber processing equipment, b) CNT – polymer hybrid nonwoven fabrics created with varying weight percentages of CNTs, c) SEM image of the 30% CNT hybrid fabric shows an order of magnitude size difference between CNTs and electrospun nanofibers, d) SEM image showing the same hybrid after calendaring with the melted nanofibers bonding the CNTs together.

properties of the hybrid fabrics which were consolidated under pressure are presented in Figure 3b. All of the consolidated samples increased in strength, but the pure consolidated electrospun material still exhibited very low mechanical properties. Among the consolidated hybrid fabrics, the 30% CNT hybrid fabric exhibited the highest tensile strength which was 21x higher than the electrospun control sample. It is likely that the applied pressure created more direct contacts between CNTs and PEO nanofibers which provided better load transfer to the CNTs. Figure 3c shows that the tensile strength of the hybrid fabrics increased dramatically after calendaring. Tensile strength of the 15% CNT hybrid fabric increased to 75 MPa, while the 30% CNT hybrid fabric exhibited a tensile strength of 172 MPa which was 49x higher than the electrospun control and three orders of magnitude greater than the as-produced PEO nanofiber fabric. The specific tensile strengths of the fabrics are shown in Figure 3d. The as-produced and consolidated 60% CNT hybrid fabrics exhibited the highest specific strength due to its lower density (Table S2, Supporting Information). After heated calendaring, the specific strength of 30% CNT hybrid fabric increased to 239 MPa/gcm⁻³ which is 60x higher than the control sample. In general, when the CNT ratio increased in the hybrid fabric, the specific strength went up, because CNTs are the stronger component and the CNT sheet structure has lower packing density compared to electrospun fibers.

While it was no surprise that the CNTs would reinforce the electrospun fabrics it was also found that the polymer nanofibers were critical to enhancing load transfer between CNTs. The hybrid

structures were all significantly stronger than the 100% CNT control fabrics. It should also be noted that even though the in-plane mechanical properties of the calendared fabrics increased significantly, they maintained excellent flexibility and conformability.

Commercial nonwoven fabrics, which contain drawn microfibrils, are much stronger than fabrics made exclusively from nanofibers. One of the goals of the nonwovens industry is to make stand alone nanofiber fabrics which have similar mechanical properties to their commercial products. Using our technique, it appears that this goal is attainable. A comparison of the CNT-nanofiber hybrid fabrics to traditional thermally bonded microfibril nonwoven fabrics is shown in Figure 3e. Units are given in grams per tex which is a textile unit of specific strength typically used to quantify strength of nonwoven fabrics. Before calendaring, the fabrics strengths were on par with the common range of values found for thermally bonded nonwoven fabrics. After calendaring, the fabrics' specific strength increased significantly and was larger than thermally bonded nonwoven fabrics found in the literature^[47-53]

Figure 3f shows the summary of our results next to other examples of CNT reinforced polymer nanofiber fabrics produced using the electrospinning technique. Many research groups have tried to improve the mechanical and electrical properties of electrospun webs by dispersing short CNTs into the spinning solution^[27,28]. Due to dispersion issues, a maximum loading of a few weight percent is possible with this method. The resulting fabrics typically show an increase in mechanical properties, but have been

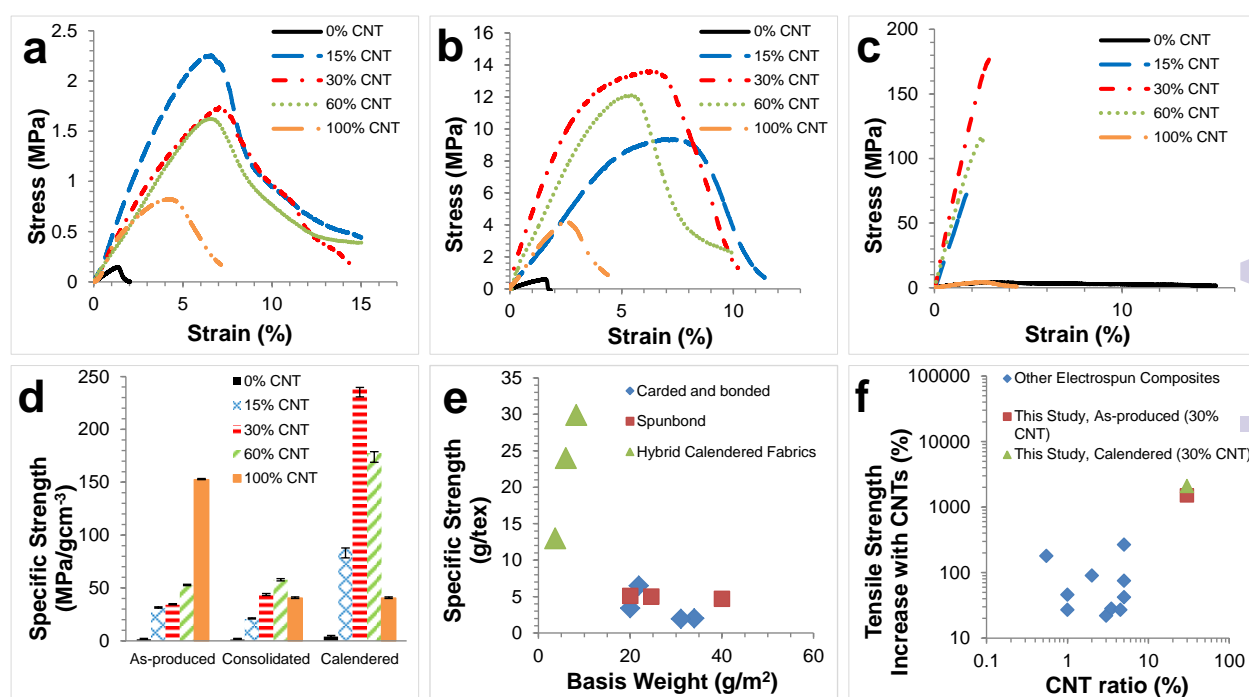


Fig. 3 (a) Tensile mechanical properties of the as-produced hybrid fabrics with different CNT loadings, (b) Tensile mechanical properties of the hybrid fabrics after consolidation under pressure, (c) Tensile mechanical properties of the hybrid fabrics after calendaring at 70 °C, (d) Comparison of specific strength between control sample and hybrid fabrics, (e) Comparison of the mechanical properties for the 15%, 30% and 60% calendared CNT hybrid fabrics to thermally bonded nonwovens from references^[47-53]. Specific strength increased with increasing CNT content, (f) Strength increases seen for our hybrids as compared to electrospun fabrics with CNTs in the spinning solution from references^[7,22,25,28,29,34,40,46,54,73].

limited to a maximum increase in strength of 4x and typically much lower gains are observed^[25,26,29,54]. Using our process however, we have seen strength increases in our material of up to 49x due to the addition of the CNTs. This is mainly attributed to the large CNT aspect ratios and the much higher CNT loading levels.

Electrical conductivity of hybrid fabrics is shown in Figure 4. It was measured using a 4-probe setup where the fabrics were laid across four sputtered gold electrodes. The results showed that as-produced hybrid fabrics had similar conductivity. This result proved that even though nonconductive polymer nanofiber layers were deposited in between layers of the CNT sheet, a number of CNTs were still able to make electrical contact allowing every CNT sheet layer to contribute to the conductivity. Even the hybrid with 15% CNTs showed electrical conductivity. After consolidation under pressure, the electrical conductivity increased to 50 S/cm for 30% and 60% CNT hybrid fabrics. However, since the interconnection between the layers was likely lower for the 15% CNT hybrid fabric, the electrical conductivity did not increase as much as the other consolidated hybrid fabrics. When hybrid fabrics were calendared, electrospun fibers between CNT layers melted and the CNT interconnections reached a maximum level while the thickness was decreased. This increased the electrical conductivity to 205 S/cm for the 60% CNT hybrid fabric. After consolidation, the pure CNT sheet exhibited an electrical conductivity of 115 S/cm meaning that the 60% CNT hybrid fabric showed higher electrical conductivity than pure consolidated CNTs. We hypothesized that after calendaring the hybrid fabrics, the polymer shrank and helped the CNTs to come into closer permanent contact with each other. This behavior has also been reported previously in the literature by others that have melted polymer-CNT assemblies^[55].

3.3 Aerosol Filtration Results

One of the major applications of nanofiber fabrics is in air filtration. Electrospun nanofibers typically show a significant advantage in aerosol filtration efficiency due to their large specific surface area and small pore size in comparison to commercial textiles^[1,2]. However their lower tensile strength means that they have to be used with supporting nonwoven fabrics^[56,57]. Recently it was shown that filters containing aligned CNT sheets also exhibit excellent filtration properties. The CNTs have smaller fiber diameters and higher filtration efficiencies at lower pressure drops compared to electrospun fibers^[44]. CNTs must be permanently trapped in the fabric so that they act only as a filtering agent^[44]. The CNT-nanofiber hybrid fabrics show high potential in the area of filtration because they work around many of the disadvantages of CNT and nanofiber based filters.

Figure 5 shows filtration performance of CNT – polymer hybrid nonwoven fabrics, in terms of the particle penetration percentage, for the standard 10-300 nm particle size range tested. There are three basic mechanisms that lead to capture of an aerosol particle in neutral fibrous filters: interception, inertial impaction and Brownian diffusion. The total particle collection efficiency of a filter is the combination of these three capturing mechanisms^[58,59]. Overall filtration performance is a function of the fiber diameter, packing density, filter thickness, and the sum of single fiber efficiencies due to these three different deposition mechanisms^[57]. The filtration performance of 7-layer CNT – polymer hybrid nonwoven fabrics with different CNT loadings are shown in Figure 5a. The penetration for the control sample was 10.54%, while the 60% CNT hybrid fabric decreased penetration to 0.024% at the 0.3 μm particle size. The 15% CNT hybrid fabric decreased penetration

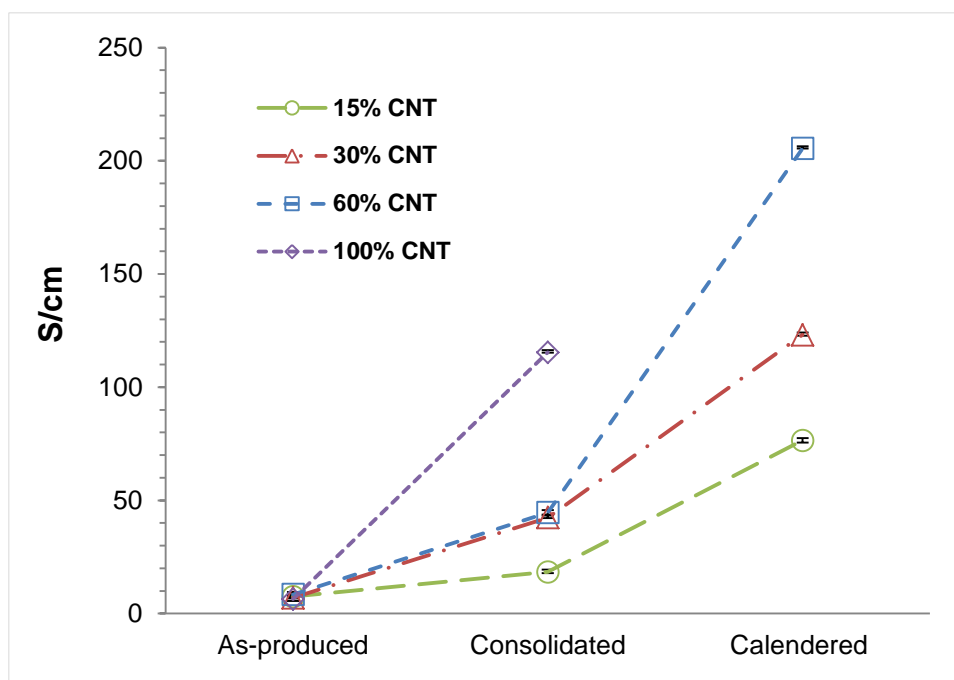


Fig. 4. Electrical conductivity of the as-produced, consolidated and calendared hybrid fabrics and pure as-produced and consolidated CNT sheet samples.

one more order to 0.0019% at the 0.3 μm particle size due to more electrospun fibers in the hybrid fabric (lower mandrel rotation speed but same number of total rotations). Due to the small diameters of CNTs, the most penetrating particle size (MPPS) of hybrid fabrics was around 70 nm which is lower than for conventional micro fibers^[57]. While the specific surface area of each sample was not measured, it is clear that the addition of large weight fractions of CNTs to the hybrids increased the overall surface area of the fabrics and reduced the average pore size, which enhanced the filtration efficiency in diffusion regime^[58].

Filtration of ultrafine particles is accomplished by using HEPA (high efficiency particulate air) or ULPA (ultra-low penetration air) filters. The requirement for a HEPA filter is at least 99.97% filtration efficiency at the 0.3 μm particle size. The ULPA designation requires at least 99.999% filtration efficiency of particles 0.12 μm particle or larger^[44]. All the as-produced hybrid fabrics reached the HEPA filter standards and the 15% CNT consolidated hybrid fabric met the ULPA filter requirements with the value of 0.0019% penetration at

0.1 μm particle size, as seen in Figure 5b. This was achieved with a fabric with a thickness of only 20 microns and areal density of 8 g/m^2 .

Pressure drop is another important parameter for aerosol filter. A low pressure drop is always a desired filtration property due to energy requirements in large scale of filtration process. Fiber diameter, thickness of the filter media, fiber packing density, and face velocity directly affect pressure drop^[44]. Figure 5c shows the particle penetrations versus pressure drops of as-produced and consolidated hybrid fabrics at 15 cm/s face velocity. The as-produced hybrid fabrics showed a lower pressure drop compared to the consolidated hybrids due to decreased pore sizes and high packing density after consolidation.

It is desirable to have the highest filtration efficiency and the lowest pressure drop in any filter. Filter quality factor (QF) is a parameter used to compare filter types and filters of varying thickness, and is a ratio between filtration efficiency and pressure drop^[44,56].

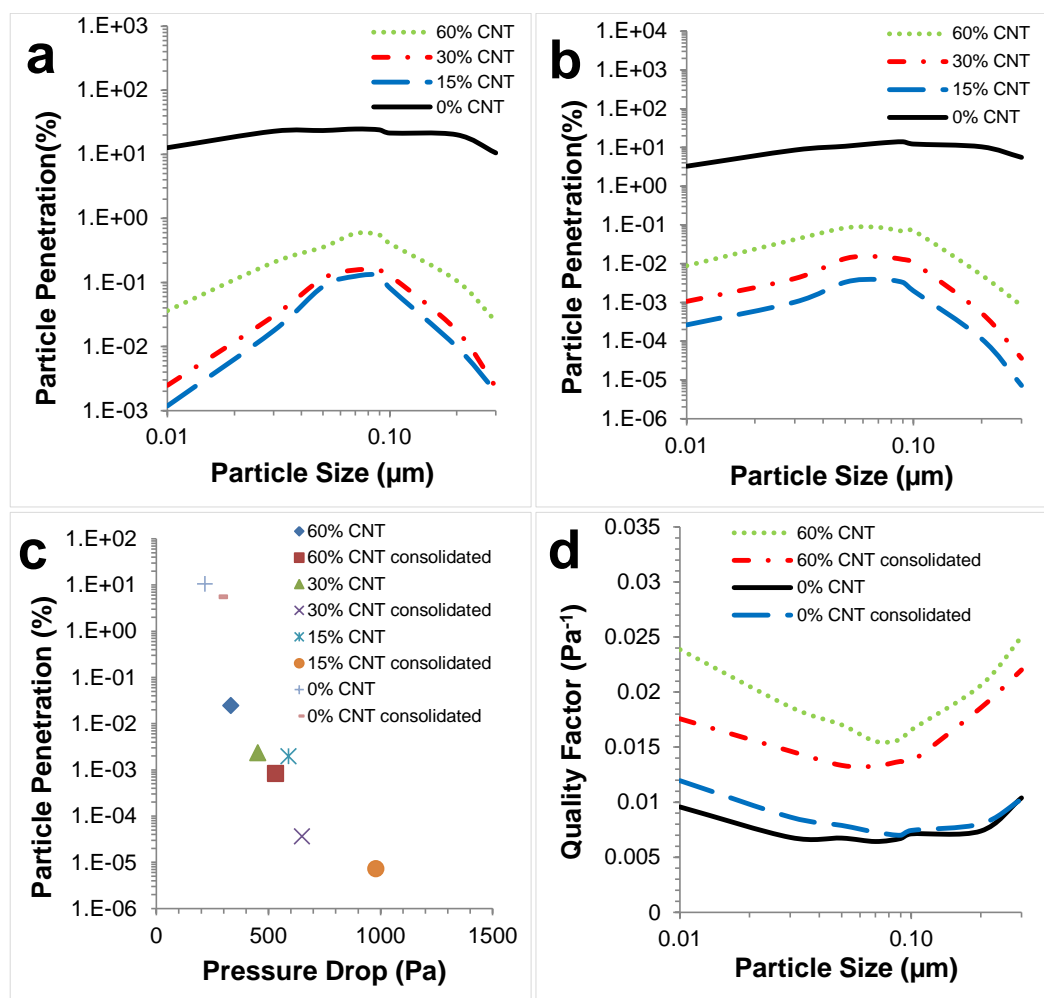


Fig. 5 (a) The hybrid fabrics with different CNT fiber loading, evaluated for particle penetration for a range of particle sizes at a face velocity of 15 cm/s , (b) The hybrid fabrics with different CNT fiber loading after consolidated under pressure, evaluated for particle penetration for a range of particle sizes at a face velocity of 15 cm/s , (c) Particle penetration fraction of the hybrid fabrics at different CNT fiber loading before and after consolidation as a function of pressure drop at 0.3 μm particle size and 15 cm/s face velocity, (d) Quality factor as a function of DOP particle size, ranging from 0.01 to 0.3 μm , at 15 cm/s face velocity.

$$QF = -\frac{\ln P}{\Delta p} \quad \text{Equation (2)}$$

where P is the filter penetration and Δp is the pressure drop. The most efficient filter is the one that has the greater value of QF . Figure 5d shows the comparison of the QF between the 60% CNT hybrid fabrics and the control samples before and after consolidation. The as-produced and consolidated control samples both had the lowest QF . The QF of the 60% CNT hybrid fabrics was significantly higher because their filtration efficiency increases were more significant than the pressure drop increases.

The calendered hybrid fabrics showed much higher pressure drop making them less attractive for filtration applications. However, at the 60% CNT loading level the fabric appeared very porous making this material attractive for micro-porous membranes. Micro-porous membranes and laminated fabrics, are used as barrier materials for protective clothing applications, and can provide a high level of protection from liquids while still allowing water vapor to escape^[5,6,60–62]. However, these types of fabrics typically have lower water vapor permeability which lowers the comfort level for the wearers^[5,6,61]. Therefore, the most common expectations from barrier materials for protective clothing applications are a combination of adequate barrier performance and comfort, simultaneously^[5,6,60]. Electrospun nonwoven mats have improved breathable barrier fabric properties due to high specific surface area, high porosity and small pore sizes. However, since electrospun nonwoven mats have low mechanical properties, they are commonly laminated on to thicker supporting fabrics which may affect the barrier and comfort performance of the final material^[61,63].

The unique combination of high specific surface area, flexibility, light weight, and porous structure with the desired level of high tensile strength makes these CNT – polymer hybrid nonwoven fabrics excellent candidates for use in stand alone barrier fabrics for protective garments. Figure 6 shows the barrier and water vapor

permeability performance of hybrid fabrics. The water vapor permeability (MVP) of the 7-layer 60% CNT hybrid fabrics in the different structures (as-produced, consolidated, and calendered) shown in Figure 6a. All the CNT hybrid fabric samples showed essentially the same moisture vapor transmission rate (MVTR). However, the as-produced hybrid fabric showed higher MVP compared to consolidated and calendered samples, because the as-produced hybrid fabric had a larger thickness which directly affects the MVP value.

In order to improve the hybrid fabrics performance against chemical agents, the hybrid sheets were treated with a low surface energy chemical, perfluorooctylethyl acrylate^[64] (PFAC8, 1) using pulsed polymerization.



Pulsed plasma polymerisation of PFAC8 on the microsecond-millisecond timescale has been shown to produce a polymer with high levels of structural integrity^[65]. The greater control associated with this technique is due to the limited fragmentation that occurs during the “on” time of the pulse sequence and the conventional gas phase chemistry that occurs during the “off” period. By varying the “on” and “off” times and the radio frequency power level, the process may be optimized and the desired surface characteristics obtained^[66–68].

Pulsed plasma polymerisation of PFAC8 occurs predominantly via its acrylic double bond, depositing a polymer that resembles conventional poly(PFAC8) produced by liquid phase free-radical polymerisation. Once applied to the fiber surfaces of the hybrid materials, the perfluoroalkyl chains in the outermost layer of the thin polymer film orientate themselves normal to the fiber surface, forming a sheath of closely-packed CF_3 -terminated perfluoroalkyl groups^[65]. The critical surface tension and surface energy values of this structure are exceedingly low (ca 4 mNm^{-1} and 8 mJm^{-2} respectively)^[66,69], resulting in remarkable liquid-repellent

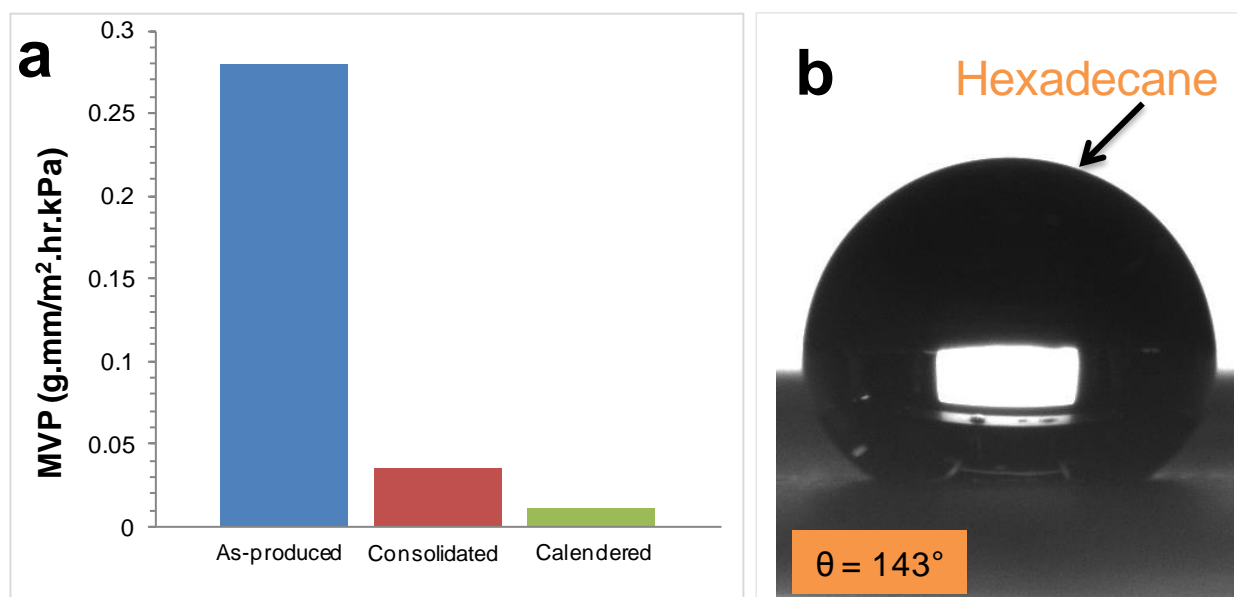


Fig. 6 a) MVP results for hybrid fabrics, b) A droplet of hexadecane on a 60% CNT consolidated hybrid fabric.

properties, especially when applied to fibrous substrates^[64,70,71]. After the plasma treatment, contact angle measurements were made using a series of probe liquids consisting of water, hexadecane, ethylene glycol and di-iodomethane (Table S3, Supporting Information). A droplet of hexadecane on a 60% CNT consolidated hybrid fabric is shown in Figure 6b. The contact angle is very high for such a low surface tension organic liquid. The very high contact angle of 143° is attained through a combination of the extremely porous nano-fiber surface and the low surface energy coating^[72]. The combination of high water vapor permeability and protection against harmful liquid chemicals make these hybrid fabrics excellent candidates for chemical protective garments⁷⁴.

4. Conclusions

In summary, we have developed a novel process to produce nanoscale nonwovens through a hybridization of high aspect ratio CNTs and electrospun fabrics, which were processed in a way that is conducive to future commercial production. Due to the unique properties of the CNTs, the hybrids showed extremely high tensile strength, small pore size, high specific surface area and electrical conductivity. In order to further examine hybrids properties, they were consolidated under pressure, and also calendared at 70 °C. The hybrid fabrics remained porous even after calendaring and look similar to thermally spot bonded nonwoven fabrics. After heated calendaring, the fabrics' strength increased immensely due to better bonding and interconnection with the CNTs. The specific strength values were larger than for any thermally bonded nonwoven fabrics found in the literature. The fabrics also exhibited very good particle filtration and barrier properties. These novel hybrid fabrics may be desirable as stand alone fabrics in applications such as aerosol and liquid filtration, protective garments, barrier membranes, tissue scaffolds and catalyst support structures. PEO was utilized as the polymer nanofiber in these hybrid fabrics, however, the technology can easily be extended to many other polymer/fiber systems in future studies.

Acknowledgements

The authors acknowledge the Turkish Ministry of National Education for provision of a Ph.D. scholarship to Ozkan Yildiz, and Dr. Yuntian Zhu at NC State University for use of the Shimadzu mechanical tester machine. The authors acknowledge the use of the Analytical Instrumentation Facility (AIF) at North Carolina State University, which is supported by the State of North Carolina and the National Science Foundation. The authors also thank Engin Kapkin for assistance with illustrations.

References

- 1 Y. C. Ahn, S. K. Park, G. T. Kim, Y. J. Hwang, C. G. Lee, H. S. Shin, J. K. Lee, *Curr. Appl. Phys.*, 2006, **6**, 1030–1035.
- 2 G. T. Kim, Y. C. Ahn, J. K. Lee, *Korean J. Chem. Eng.*, 2008, **25**, 368–372.
- 3 S. S. Homaeigohar, K. Buhr, K. Ebert, *J. Memb. Sci.*, 2010, **365**, 68–77.

- 4 R. Gopal, S. Kaur, Z. Ma, C. Chan, S. Ramakrishna, T. Matsuura, *J. Memb. Sci.*, 2006, **281**, 581–586.
- 5 L. Chen, L. Bromberg, H. Schreuder-Gibson, J. Walker, T. Hatton, G. C. Rutledge, *J. Mater. Chem.*, 2009, **19**, 2432–2438.
- 6 R. Bagherzadeh, M. Latifi, S. S. Najari, M. A. Tehran, M. Gorji, L. Kong, *Text. Res. J.*, 2011, **82**, 70–76.
- 7 H. Liao, R. Qi, M. Shen, X. Cao, R. Guo, Y. Zhang, X. Shi, *Colloids Surf. B. Biointerfaces*, 2011, **84**, 528–535.
- 8 D. Hussain, F. Loyal, A. Greiner, J. H. Wendorff, *Polymer*, 2010, **51**, 3989–3997.
- 9 L. Huang, J. T. Arena, S. S. Manickam, X. Jiang, B. G. Willis, J. R. McCutcheon, *J. Memb. Sci.*, 2014, **460**, 241–249.
- 10 J. Yao, C. W. M. Bastiaansen, T. Peijs, *Fibers*, 2014, **2**, 158–187.
- 11 B. Ding, E. Kimura, T. Sato, S. Fujita, S. Shiratori, *Polymer*, 2004, **45**, 1895–1902.
- 12 Z.-M. Huang, Y.-Z. Zhang, M. Kotaki, S. Ramakrishna, *Compos. Sci. Technol.*, 2003, **63**, 2223–2253.
- 13 C. Huang, S. Chen, D. H. Reneker, C. Lai, H. Hou, *Adv. Mater.*, 2006, **18**, 668–671.
- 14 C.-L. Pai, M. C. Boyce, G. C. Rutledge, *Polymer*, 2011, **52**, 6126–6133.
- 15 J.-S. Kim, D. H. Reneker, *Polymer Engineering and Science*, 1999, **39**, 849–854.
- 16 X. Wang, K. Zhang, M. Zhu, B. S. Hsiao, B. Chu, *Macromol. Rapid Commun.*, 2008, **29**, 826–831.
- 17 Y. Lee, B.-S. Kim, J. H. Hong, S. Park, H. Kim, I.-S. Kim, *J. Polym. Res.*, 2012, **19**, 9774.
- 18 G. H. Kim, *Biomed. Mater.*, 2008, **3**, 025010.
- 19 J. H. Hong, E. H. Jeong, H. S. Lee, D. H. Baik, S. W. Seo, J. H. Youk, *J. Polym. Sci. Part B Polym. Phys.*, 2005, **43**, 3171–3177.
- 20 Z. Ma, M. Kotaki, S. Ramakrishna, *J. Memb. Sci.*, 2006, **272**, 179–187.
- 21 J. Liu, Z. Yue, H. Fong, *Small*, 2009, **5**, 536–542.
- 22 R. Sen, B. Zhao, D. Perea, M. E. Itkis, H. Hu, J. Love, E. Bekyarova, R. C. Haddon, *Nano Letters*, 2004, **4**, 459–464.
- 23 G. M. Kim, R. Lach, G. H. Michler, P. Pötschke, K. Albrecht, *Nanotechnology*, 2006, **17**, 963–972.
- 24 J. J. Mack, L. M. Viculis, A. Ali, R. Luoh, G. Yang, H. T. Hahn, F. K. Ko, R. B. Kaner, *Adv. Mater.*, 2005, **17**, 77–80.
- 25 S. Mazinani, A. Ajji, C. Dubois, *Polymer*, 2009, **50**, 3329–3342.
- 26 S. Mazinani, A. Ajji, C. Dubois, *J. Polym. Sci. Part B Polym. Phys.*, 2010, **48**, 2052–2064.
- 27 M. V. Jose, B. W. Steinert, V. Thomas, D. R. Dean, M. A. Abdalla, G. Price, G. M. Janowski, *Polymer*, 2007, **48**, 1096–1104.
- 28 H. Hou, J. J. Ge, J. Zeng, Q. Li, D. H. Reneker, A. Greiner, S. Z. D. Cheng, *Chem. Mater.*, 2005, **17**, 967–973.
- 29 L. Cao, D. Su, Z. Su, X. Chen, *Ind. Eng. Chem. Res.*, 2014, **53**, 2308–2317.
- 30 M. Kang, H.-J. Jin, *Colloid Polym. Sci.*, 2007, **285**, 1163–1167.
- 31 G. Wang, Z. Tan, X. Liu, S. Chawda, J.-S. Koo, V. Samuilov, M. Dudley, *Nanotechnology*, 2006, **17**, 5829–5835.

- 32 G. Mathew, J. P. Hong, J. M. Rhee, H. S. Lee, C. Nah, *Polym. Test.*, 2005, **24**, 712–717.
- 33 L.-Q. Liu, D. Tasis, M. Prato, H. D. Wagner, *Adv. Mater.*, 2007, **19**, 1228–1233.
- 34 D. Chen, T. Liu, X. Zhou, W. C. Tjiu, H. Hou, *J. Phys. Chem. B*, 2009, **113**, 9741–9748.
- 35 X.-M. Sui, S. Giordani, M. Prato, H. D. Wagner, *Appl. Phys. Lett.*, 2009, **95**, 233113.
- 36 A. Agic, B. Mijovic, *J. Text. Inst.*, 2006, **97**, 419–427.
- 37 J. S. Jeong, S. Y. Jeon, T. Y. Lee, J. H. Park, J. H. Shin, P. S. Alegaonkar, A. S. Berdinsky, J. B. Yoo, *Diam. Relat. Mater.*, 2006, **15**, 1839–1843.
- 38 L. Y. Yeo, J. R. Friend, *J. Exp. Nanosci.*, 2006, **1**, 177–209.
- 39 K. A. Narh, L. Jallo, K. Y. Rhee, *Polymer Composites*, 2008, **29**, 809–817.
- 40 J. Ji, G. Sui, Y. Yu, Y. Liu, Y. Lin, Z. Du, S. Ryu, X. Yang, *J. Phys. Chem. C*, 2009, **113**, 4779–4785.
- 41 S. D. Mccullen, D. R. Stevens, W. A. Roberts, S. S. Ojha, L. I. Clarke, R. E. Gorga, *Macromolecules*, 2007, **40**, 997–1003.
- 42 S. S. Ojha, D. R. Stevens, K. Stano, T. Hoffman, L. I. Clarke, R. E. Gorga, *Macromolecules*, 2008, **41**, 2509–2513.
- 43 S. Faraji, K. Stano, C. Rost, J.-P. Maria, Y. Zhu, P. D. Bradford, *Carbon*, 2014, **79**, 113–122.
- 44 O. Yildiz, P. D. Bradford, *Carbon*, 2013, **64**, 295–304.
- 45 K. Fu, O. Yildiz, H. Bhanushali, Y. Wang, K. Stano, L. Xue, X. Zhang, P. D. Bradford, *Adv. Mater.*, 2013, **25**, 5109–5114.
- 46 J. H. Kim, M. Kataoka, Y. C. Jung, Y.-I. Ko, K. Fujisawa, T. Hayashi, Y. A. Kim, M. Endo, *ACS Appl. Mater. Interfaces*, 2013, **5**, 4150–4154.
- 47 S. Limem, S. B. Warner, *Text. Res. J.*, 2005, **75**, 63–72.
- 48 H. S. Kim, B. Pourdeyhimi, P. Desai, A. S. Abhiraman, *Text. Res. J.*, 2001, **71**, 965–976.
- 49 J.-H. Lin, Z.-H. Xu, C.-H. Lei, C.-W. Lou, *Text. Res. J.*, 2003, **73**, 917–920.
- 50 K. Smith, A. A. Ogale, R. Maugans, L. K. Walsh, R. M. Patel, *Text. Res. J.*, 2003, **73**, 845–853.
- 51 D. Zhang, G. Bhat, M. Sanjiv, L. Wadsworth, *Text. Res. J.*, 1998, **68**, 27–35.
- 52 A. Rawal, S. Lomov, T. Ngo, I. Verpoest, J. Vankerrebrouck, *Text. Res. J.*, 2007, **77**, 417–431.
- 53 X. Hou, M. Acar, V. V Silberschmidt, *Journal of Engineered Fibers and Fabrics*, 2009, **4**, 26–33.
- 54 P. Lu, Y.-L. Hsieh, *ACS Appl. Mater. Interfaces*, 2010, **2**, 2413–2420.
- 55 S. Ramaswamy, L. I. Clarke, R. E. Gorga, *Polymer*, 2011, **52**, 3183–3189.
- 56 J. Wang, S. C. Kim, D. Y. H. Pui, *J. Aerosol Sci.*, 2008, **39**, 323–334.
- 57 W. W.-F. Leung, C.-H. Hung, P.-T. Yuen, *Sep. Purif. Technol.*, 2010, **71**, 30–37.
- 58 A. N. Karwa, B. J. Tatarchuk, *Sep. Purif. Technol.*, 2012, **87**, 84–94.
- 59 J. H. Park, K. Y. Yoon, H. Na, Y. S. Kim, J. Hwang, J. Kim, H. Y. Yoon, *Sci. Total Environ.*, 2011, **409**, 4132–4138.
- 60 B. Yoon, S. Lee, *Fibers Polym.*, 2011, **12**, 57–64.
- 61 S. Lee, S. K. Obendorf, *J. Appl. Polym. Sci.*, 2006, **102**, 3430–3437.
- 62 S. Lee, S. K. Obendorf, *Text. Res. J.*, 2007, **77**, 696–702.
- 63 S. Lee, S. K. Obendorf, *Fibers Polym.*, 2007, **8**, 501–506.
- 64 H. J. Lee, C. R. Willis, C. A. Stone, *J. Mater. Sci.*, 2011, **46**, 3907–3913.
- 65 S. R. Coulson, I. S. Woodward, J. P. S. Badyal, S. A. Brewer, C. Willis, *Chem. Mater.*, 2000, **12**, 2031–2038.
- 66 S. R. Coulson, I. S. Woodward, J. P. S. Badyal, S. A. Brewer, C. Willis, *Langmuir*, 2000, **16**, 6287–6293.
- 67 E. J. Kinmond, S. R. Coulson, J. P. S. Badyal, S. A. Brewer, C. Willis, *Polymer*, 2005, **46**, 6829–6293.
- 68 C. Tarducci, E. J. Kinmond, J. P. S. Badyal, S. A. Brewer, C. Willis, *Chem. Mater.*, 2000, **12**, 1884–1889.
- 69 D. A. Lamprou, J. R. Smith, T. G. Nevell, E. Barbu, C. Stone, C. R. Willis, J. Tsibouklis, *Appl. Surf. Sci.*, 2010, **256**, 5082–5087.
- 70 S. A. Brewer, C. R. Willis, *Appl. Surf. Sci.*, 2008, **254**, 6450–6454–5760.
- 71 R. Saraf, H. J. Lee, S. Michielsen, J. Owens, C. Willis, C. Stone, E. Wilusz, *J. Mater. Sci.*, 2011, **46**, 5751–5760.
- 72 H. Bellanger, T. Darmanin, E. Taffin De Givenchy, F. Guittard, *Chem. Rev.*, 2014, **114**, 2694–2716.
- 73 M. Naebe, T. Lin, W. Tian, L. Dai, X. Wang, *Nanotechnology*, 2007, **18**, 225605.
- 74 H. J. Lee, C. R. Willis, *Chemistry and Industry*, 2009, **13**, 21–23